The Influence of Experimental Conditions on the Formation of ZnO Fibers by Electrospinning[†]

Mira Ristić,* Marijan Marciuš, Željka Petrović, Mile Ivanda, and Svetozar Musić

Ruđer Bošković Institute, Bijenička cesta 54, P.O. Box 180, HR-10002, Zagreb, Croatia

Abstract. The influence of experimental conditions on the formation of ZnO fibers by electrospinning has been investigated. The electrospinning of a viscous suspension containing polyvinylpyrrolidone and zinc acetate in C_2H_5OH/H_2O produced very long fibers (several hundred μm). Upon calcination a thin deposit of precursor fibers at 400 or 500 °C for 1 h the fibers consisting of ZnO nanoparticles were obtained. On the other hand, ZnO fibers were not obtained upon heating a thick deposit of precursor fibers at 600 °C for 6 h. At all three heating temperatures (400, 500 or 600 °C) ZnO nanoparticles with a gradual increase in size were produced. The Raman spectrum of ZnO nanoparticles formed at 600 °C showed additional bands which were assigned to graphene oxide. It was suggested that in the thick deposit the organic component did not burn out completely, *i.e.*, the residual carbon (graphite) transformed into graphene oxide for the experimental conditions applied.

Keywords: ZnO fibers, graphene oxide, electrospinning, electron microscopy, Raman spectroscopy, X-ray diffraction

INTRODUCTION

In recent years many researchers have strongly focused on the synthesis of zinc oxide (ZnO) particles and their properties due to the importance of this material in advanced technologies, for example in the manufacture of photovoltaic devices, LED's, transistors, sensors, varistors, *etc.* We have systematically investigated[1–9] the impact of different experimental conditions on the properties of ZnO powders. In continuation of these works we have studied the impact of experimental conditions on the formation of ZnO fibers using the electrospinning method. Generally, in this electrostatic processing method the high-voltage electric field is used to form solid fibers from a fluid (solution, suspension or melt) injected through the nozzle (1 mm or less in diameter).

Some selected works on the ZnO synthesis using electrospinning will be cited herein. For example, ZnO nanofibers were synthesized by electrospinning and tested as sensors for NO_2 and CO or NO gases.[10,11] ZnO nanofibers doped with Cu were tested[12] as a sensor for H_2S and doped[13] with Al as a sensor for C_2H_5OH. The sensitivity to C_2H_2 gas of the electrospun Ni-doped ZnO nanofibers was investigated.[14] The sensitivity of ZnO-based sensors is influenced by the specific surface area and porosity. These properties can be optimized using the electrospinning method.

The electrical properties of FE transistors based on single ZnO or Ga-doped ZnO nanofiber were also investigated.[15,16] The efficiency of organic/inorganic photovoltaic devices was improved by using the electrospun ZnO nanofibers.[17] Electrospun nanofibers forming p-type NiO/n-type ZnO heterojunctions were characterized by enhanced photovoltaic activity.[18] More information about the electrospinning method and its capabilities in the production of different fibers is given in the book by Ramakrishna *et al.*[19]

The synthesis of ZnO fibers by electrospinning depends on various factors, such as the starting zinc salt, the type of polymer or solvent, chemical concentrations, as well as the physical conditions of the experiment. In the present work some of these factors were studied with a view to obtaining more data on the formation of ZnO fibers by electrospinning.

EXPERIMENTAL

Chemicals and Sample Preparation

The following chemicals were used: polyvinylpyrrolidone (PVP, M_w = 1 300 000) supplied by *Alfa Aesar®*, zinc acetate dihydrate ($Zn(CH_3COO)_2 \cdot 2H_2O$) supplied by *Kemika* and absolute ethanol supplied by *Carlo Erba*. Twice-distilled water was prepared in own laboratory.

Sample S1 was prepared as follows. 3 g PVP was dissolved in 50 ml of absolute C_2H_5OH and 5 ml H_2O. This was continued by mixing at 350 rpm and 70 °C for 2 hours. A viscous solution was obtained.

Sample S2 was prepared by dissolving 3 g PVP in 50 ml of absolute C_2H_5OH and mixing at 250 rpm and 60 °C for 2 h. 1.2 g of zinc acetate dihydrate was dissolved in 5 ml H_2O, then added to the ethanolic solution of PVP and additionally mixed at 250 rpm and 60 °C for 3 h.

The electrospun fibers (sample S2) were calcined at 400 °C for 1 h (S2-400), 500 °C for 1 h (S2-500) and 600 °C for 6 h (S2-600). Calcination of the electrospun fibers was performed in the laboratory oven in air starting from room temperature and kept at the desired temperature for given period of time.

**Electrospinning Device and Sample Characterization**

The electrospinning device was homemade. The viscous liquid was pressed by air (15 mbar) in a glass tube capped with a nozzle (internal diameter 0.8 mm). The metallic nozzle was connected to the negative terminal of power supply adjusted at 20 kV, whereas the positive one was grounded and connected with the aluminium plate sized 15 cm × 20 cm. In the electrospinning experiments the aluminium plate was covered with aluminium foil for collecting the electrospun material. The distance between the metallic nozzle tip and the aluminium plate was 20 cm. The high-voltage auto-reserving power supply CZE 1000R manufactured by *Spellman* (N.Y., USA) was used. The electrospinning unit was installed in the plexiglas tube, 100 cm long and 50 cm in diameter.

Raman spectra were recorded using a *Horiba Jobin Yvon* spectrometer (model T64000). The measurement temperature was regulated by a THMS600 unit manufactured by *Lincam Scientific Instruments*. The argon laser beam of 514.5 nm was used as excitation source. Also used was a *Perkin-Elmer* FT-IR spectrometer (model 2000). The specimen was pressed into tablets using a spectroscopically pure KBr matrix and a *Carver* press. *ItalStructures* XRD diffractometer (model APD 2000) was used to identify the phase composition. The shape and size of fibers (particles) were inspected with a *Jeol* thermal field emission scanning electron microscope (FE-SEM, model JSM-7000F). The FE-SEM was coupled with an *Oxford Instruments* EDS/ INCA 350 (energy dispersive X-ray analyzer). The inspected samples were not coated with an electrically conductive layer. Computer program ImageJ was used in processing of FE-SEM sample images to obtain particle size distributions.

RESULTS AND DISCUSSION

Figure 1 shows fibers produced by the electrospinning of a viscous PVP solution in C_2H_5OH/H_2O solvent without Zn^{2+} ions (sample S1).

Upon electrospinning of a viscous suspension containing PVP and $Zn(CH_3COO)_2$ in C_2H_5OH/H_2O solvent, the fibers, several hundred μm long were produced (sample S2; Figure 2a). Figure 2b shows these fibers at higher magnification; their diameters measured between 0.220 and 0.340 μm. Upon their heating at 400 °C or 500 °C for 1 h the produced fibers consisted of uniform ZnO nanoparticles (Figures 2c and 2d). The EDS of the selected area showed the atomic ratio Zn:O close to that of a stoichiometric ZnO composition (Figure 3a and 3b). It should be mentioned that these ZnO fibers were produced when a thin deposit of the precursor fibers on Al foil was used (30 min of electrospinning). On the other hand, no ZnO fibers were obtained when a thick layer of the precursor fibers (~25 h of electrospinning) was heated at 600 °C for 6 h. After short time of electrospinning (30 min) the fibers were formed as a thin film on Al foil (substrate), whereas the fibers produced after a long time of electrospinning (~25 h) were easily delaminated as thick foil. The particles produced at 600 °C are shown in Figure 4 (sample S2-600), and the size distributions of ZnO particles produced at 400, 500 and 600 °C are shown in Figure 5. These distributions show a gradual increase in the average ZnO particle size with an increase in the calcination temperature. At 600 °C the sintering of the particles is also seen. The present work demonstrates that the thickness of the deposited precursor fibers (short or long time of electrospinning) plays an important role in the formation of
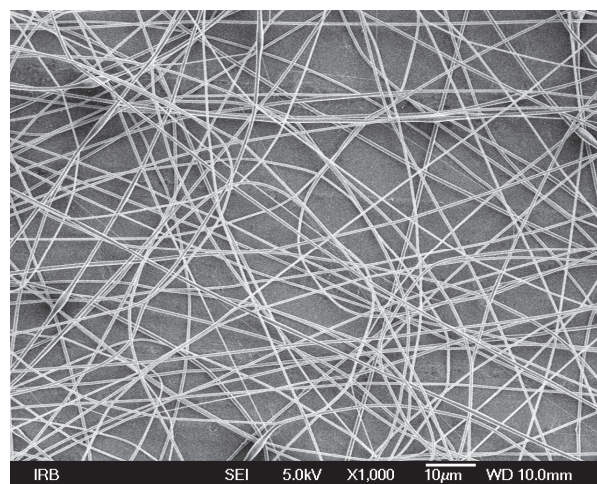
Figure 1. FE-SEM image of fibers produced by electrospinning of a viscous solution of PVP in C_2H_5OH/H_2O solvent (sample S1).
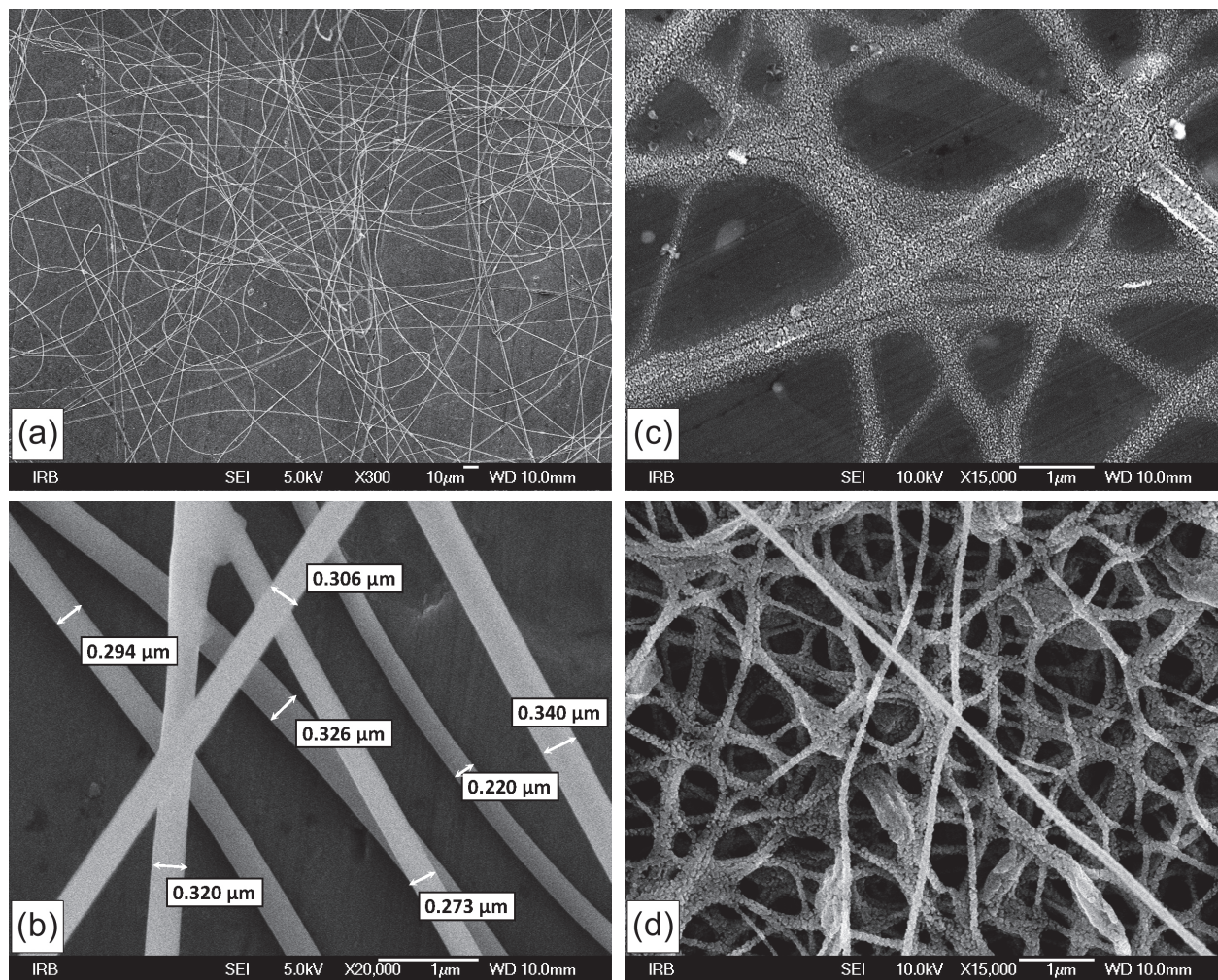
Figure 2. FE-SEM images of: sample S2 (a), sample S2 at higher optical magnification (b), sample S2-400 showing fibers consisting of uniform ZnO nanoparticles (c), and sample S2-500 showing fibers also consisting of ZnO nanoparticles (d).

ZnO fibers. Figure 6 shows the XRD pattern of particles produced at 600 °C (sample S2-600) which can be assigned to a hexagonal ZnO phase (wurtzite-type structure, space group $P6_3mc$(186); a = 0.3249 nm, c = 0.5206 nm; JCPDS card No. 36-1451).

Figure 7 shows the FT-IR spectrum of sample S2-600. The spectrum can be assigned to ZnO taking into account the result of XRD characterization of the same sample. The FT-IR spectrum of sample S2-600 is characterized by an IR band at 444 cm^{-1} and a pronounced shoulder at 486 cm^{-1}. According to Hayashi *et al.*[20] ZnO shows three distinct absorption peaks located between the bulk TO-phonon frequency (Cω_{TII}) and the LO-phonon frequency (C$\omega_{L\perp}$). The absorption peaks shifted towards lower frequencies when the permittivity of the surrounding medium was increased. The IR spectrum of ZnO particles may vary from a very broad single band over a doublet up to a three-band superposition.[21] The feature of the IR spectrum of ZnO depends on the geometrical shape of the particles.[22] Pandiyarajan *et al.*[23]

prepared ZnO by crystallizing the gel formed by adding the NaOH solution to the Zn(NO$_3$)$_2$ solution. The FT-IR spectrum displayed an IR band at 444 cm^{-1}. The IR band recorded at 454 cm^{-1} was red shifted up to 427 cm^{-1} when ZnO was doped[24] with 10 % Co. Kansal *et al.*[25] synthesized ZnO particles using the hydrothermal procedure and the corresponding FT-IR spectrum displayed an IR band positioned at ~478 cm^{-1}. Sui *et al.*[26] syntesized hexagonal ZnO prisms using a microemulsion containing PVP and these particles showed IR bands at 460–500 cm^{-1} due to Zn–O band vibration.

Samples S2-400, S2-500 and S2-600 were also investigated using Raman spectroscopy. Generally, this technique is very useful in the characterization of metal oxide particles and specifically their surfaces. Damen *et al.*[27] interpreted the Raman spectrum of ZnO. Two E_2 vibrations at 101 and 437 cm^{-1}, one transverse A_1 at 381 cm^{-1} and one transverse E_1 at 407 cm^{-1}, one longitudinal A_1 at 574 cm^{-1} and one longitudinal E_1 at 583 cm^{-1} were reported. Ristić *et al.*[4] recorded the Raman spectra of
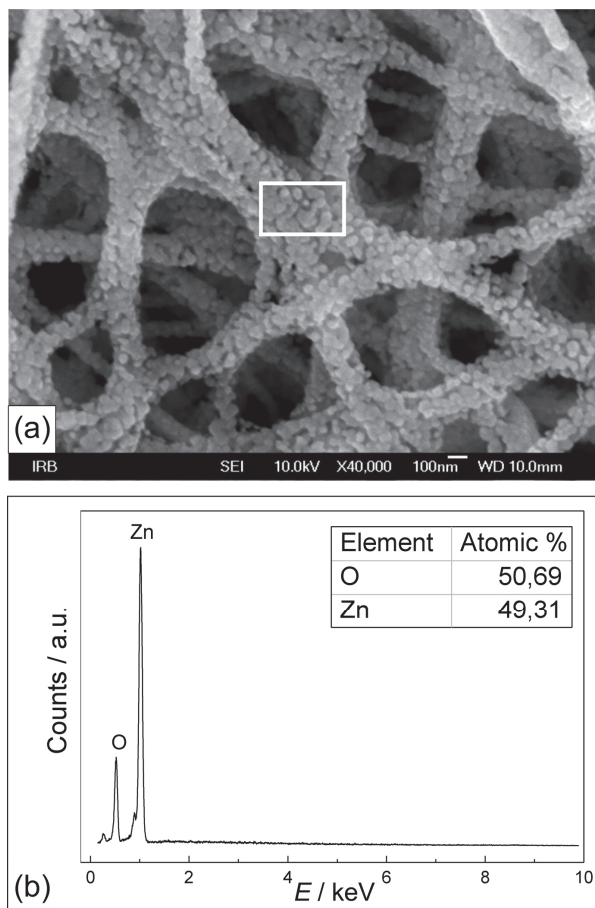
Figure 3. FE-SEM image of sample S2-500 at higher optical magnification (a) and EDS spectrum of selected area showing the atomic composition close to stoichiometric ratio Zn:O in ZnO (b).

ZnO nanoparticles produced by the sol-gel procedure and found differences in relation to the Raman spectrum of large ZnO particles. The Raman band at 392 cm^{-1} recorded for ZnO nanoparticles was noticed at 381 cm^{-1} with large ZnO particles. The Raman band at 407 cm^{-1} noticed with large ZnO particles was shifted to 418 cm^{-1} with ZnO nanoparticles. The increase in relative intensities for the Raman band at 580 cm^{-1} and the shoulder at 542 cm^{-1}, including the broadening, was likewise assigned to ZnO nanoparticles. The effect of very fine SnO$_2$ particles and their aggregation were included in the investigation of the corresponding Raman spectrum.[28] Zhao *et al.*[29] prepared In-doped ZnO particles of different morphologies and detected an influence of In-doping on the feature of the Raman spectra. Stanković *et al.*[30] investigated ZnO particles with Raman spectroscopy and the specific features in the spectra were attributed to the presence of structural defects (oxygen vacancies and zinc interstitials).

The Raman spectra of samples S2-400 and S2-500 (white films) are shown in Figure 8. These Raman spectra correspond to a pure ZnO phase.
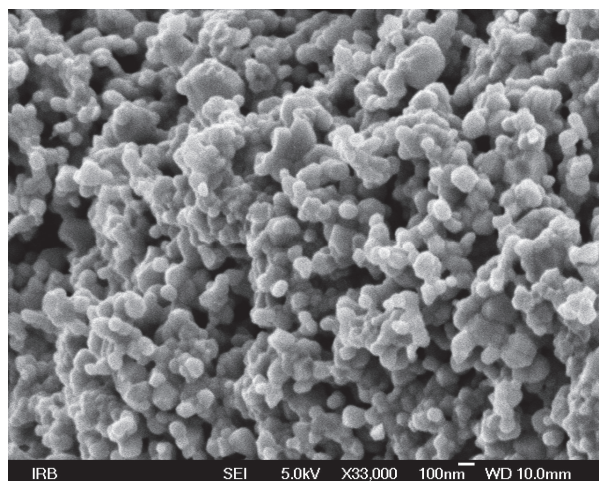

**Figure 4.** FE-SEM image of ZnO nanoparticles (sample S2-600) produced by heating sample S2 at 600 °C for 6 h.
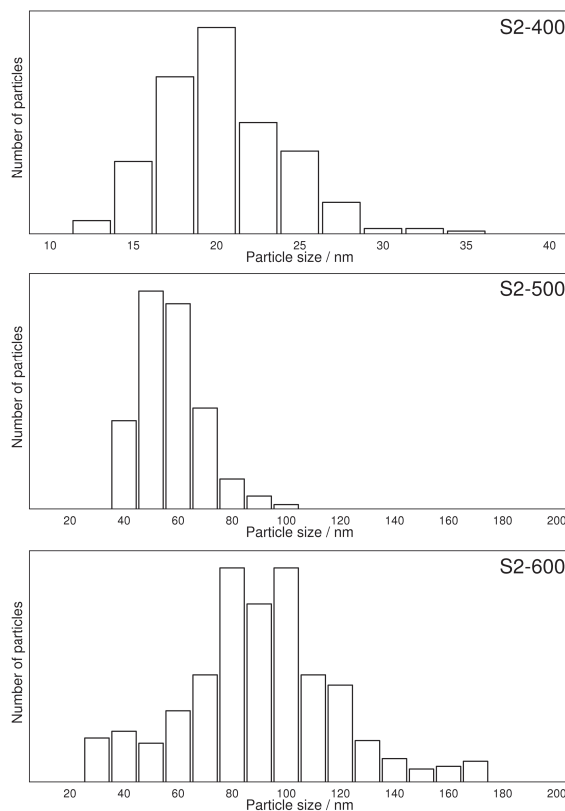
Figure 5. Size distributions of ZnO nanoparticles produced upon heating sample S2 at 400 °C (sample S2-400), 500 °C (sample S2-500) and 600 °C (sample S2-600).

The Raman spectrum of sample S2-600 is shown in Figure 9. Shown in the same figure are the Raman spectra of commercial ZnO and graphite as reference materials. In the spectral range recorded between 10 and 800 cm^{-1} all observed Raman bands are typical of a
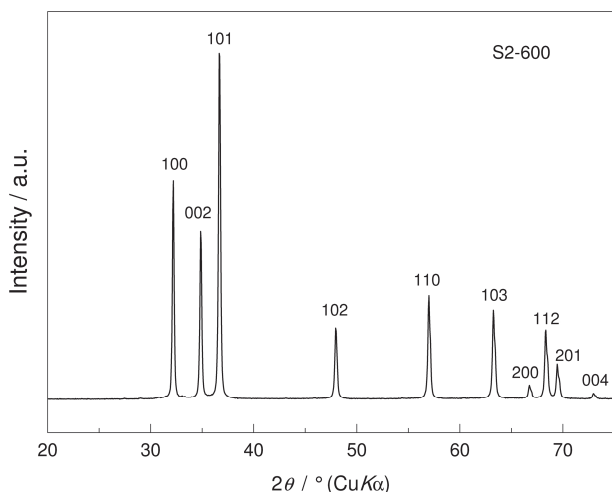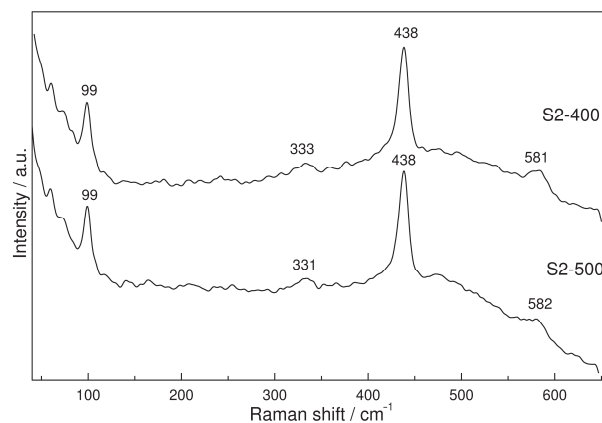
Figure 6. XRD pattern of sample S2-600.
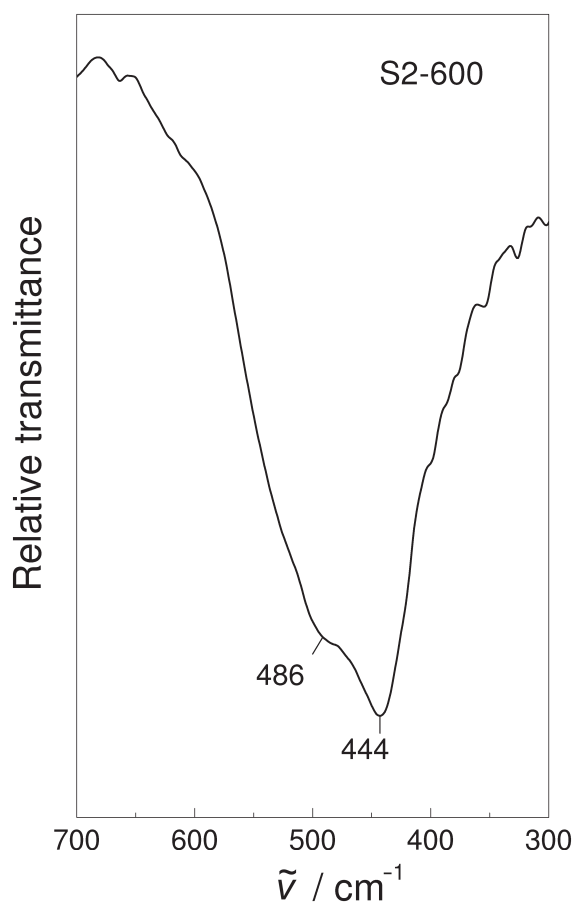
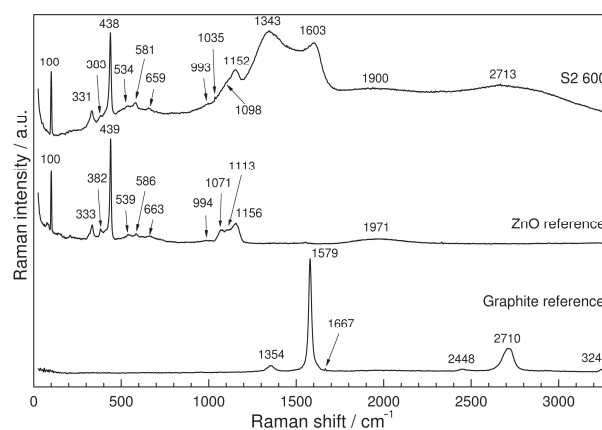**Figure 7.** FT-IR spectrum of sample S2-600.

Figure 8. Raman spectra of samples S2-400 and S2-500.

Figure 9. Raman spectrum of sample S2-600. Raman spectra of commercial ZnO and graphite as reference materials are also shown.

ZnO phase and their assignations are in line with the previous discussion. The Raman band in the spectral range 993–1152 cm^{-1} can be interpreted as the first harmonics of fundamental A_1(LO) vibrations between 534 to 659 cm^{-1} and centered at 581 cm^{-1} in the present case. However, the spectrum of sample S2-600 additionally showed very broad bands at 1343, 1603 and 2713 cm^{-1} which are not present in reference ZnO (commercial sample). Since the precursor of the sample S2-600 was a thick deposit, a possibility of carbon formation during the calcination of PVP containing fibers was supposed.. The ZnO particles of sample S2-600, obtained by heating of the thick layer of their precursor, were white-gray and this was additional motivation to inspect their surface nature. However, the formation of graphite as the main carbon-containing phase is less likely, because the XRD pattern of sample S2-600 (Figure 5) showed no intensive diffraction line (002) of graphite at $2\theta \sim 26.4$ °. It is more likely that the formation of graphene oxide (GO) is dominant due to the thick precursor deposit and the calcining conditions.

Generally, graphene possesses a two-dimensional (2D) structure consisting of sp^2 carbon network with one atom thickness. The Raman band at 1343 cm^{-1} is often interpreted as a disorder-induced D band, whereas the one at 1603 cm^{-1} as a graphite band (G). The D band
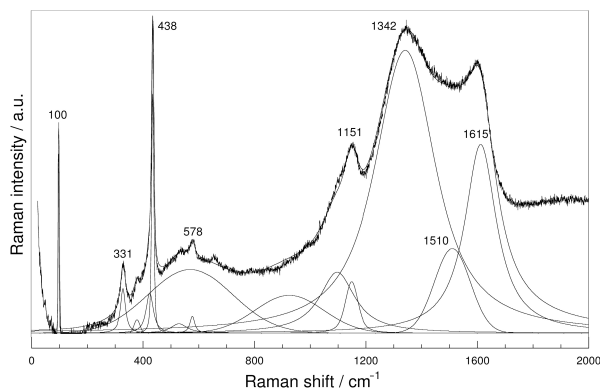
Figure 10. Deconvolution of D (disorder) and G (graphite) Raman bands, characteristic of graphene oxide (GO).

originates from structural imperfections, as A_{1g} mode, and the G band is the first-order scattering in the E_{2g} vibrational mode in graphite sheets. Due to the shape of D and G Raman bands, shown in Figure 9, they were resolved into three bands positioned at 1342, 1510, and 1615 cm^{-1} (Figure 10). Evidently, the features of D and G Raman bands, as well as the band D' at 1510 cm^{-1}, in the present case show a distribution of disorders in more GO layers with different participation of the carbon-oxygen bond. This conclusion is supported by the presence of a very broad Raman band centered at 2713 cm^{-1} (2D, D+G, 2G superposition).

CONCLUSION

- Electrospinning of a viscous suspension containing PVP and zinc acetate in C_2H_5OH/H_2O produced several hundred μm long fibers (precursor fibers)

- Fibers consisted of ZnO nanoparticles were obtained on heating a thin deposit of precursor fibers at 400 or 500 °C for 1 h

- No ZnO fibers were obtained on heating a thick deposit of precursor fibers at 600 °C for 6 h

- ZnO nanoparticles with a gradual increase in size were produced at all three heating temperatures (400, 500 or 600 °C)

- The Raman spectrum of ZnO nanoparticles formed at 600 °C showed additional bands which were assigned to graphene oxide. The organic component in a thick deposit of precursor fibers did not burn out completely at 600 °C and the residual carbon (graphite) transformed into graphene oxide film onto ZnO particles for the experimental conditions applied.

REFERENCES

1. S. Musić, S. Popović, M. Maljković, and Đ. Dragčević, *J. Alloys Comp.* **347** (2002) 324–332.
2. S. Musić, Đ. Dragčević, M. Maljković, and S. Popović, *Mater. Chem. Phys.* **77** (2002) 521–530.
3. S. Musić, Đ. Dragčević, S. Popović, and M. Ivanda, *Mater. Lett.* **59** (2005) 2388–2393.
4. M. Ristić, S. Musić, M. Ivanda, and S. Popović, *J. Alloys Comp.* **397** (2005) L1–L4.
5. S. Musić, Đ. Dragčević, and S. Popović, *J. Alloys Comp.* **429** (2007) 242–249.
6. S. Musić, A. Šarić, and S. Popović, *J. Alloys Comp.* **448** (2008) 277–283.
7. S. Musić, A. Šarić, and S. Popović, *Ceramics Int.* **36** (2010) 1117–1123.
8. A. Šarić, S. Musić, and M. Ivanda, *J. Mol. Struct.* **993** (2011) 219–224.
9. S. Musić and A. Šarić, *Ceramics Int.* **38** (2012) 6047–6052.
10. C. Lee, S.-W. Park, Y. Jae, and S. S. Kim, *Sensor Lett.* **9** (2011) 132–136.
11. O.-K. Kim, H. Kim, and D. Kim, *Korean J. Mater. Res.* **22** (2012) 609–614.
12. M. Zhao, X. Wang, L. Ning, J. Jia, X. Li, and L. Cao, *Sensors and Actuators B* **156** (2011) 588–592.
13. M. Zhao, X. Wang, J. Cheng, L. Zhang, J. Jia, and X. Li, *Current Appl. Phys.* **13** (2013) 403–407.
14. X. Wang, M. Zhao, F. Liu, J. Jia, X. Li, and L. Cao, *Ceramics Int.* **39** (2013) 2883–2887.
15. J. Y. Park, J. J. Kim, and S. S. Kim, *Microelectron. Eng.* **101** (2013) 8–11.
16. Y. Shmueli, G. E. Shter, O. Assad, H. Haick, P. Sontag, P. Ricoux, and G. S. Grader, *J. Mater. Res.* **27** (2012) 1672–1679.
17. M. Tanveer, A. Habib, and M. B. Khan, *Mater. Sci. Eng. B* **177** (2012) 1144–1148.
18. Z. Zhang, C. Shao, X. Li, C. Wang, M. Zhang, and Y. Liu, *ACS Appl. Mater. Interfaces* **2** (2010) 2915–2923.
19. S. Ramakrishna, K. Fujihara, W.-E. Teo, T.-C. Lim, and Z. Ma, *An Introduction to Electrospinning and Nanofibers*, World Scientific Publishing Co. Pte Ltd., Singapore, 2005., pp. 396.
20. S. Hayashi, N. Nakamori, H. Kanamori, Y. Yodogawa, and K. Yamamoto, *Surf. Sci.* **86** (1979) 665–671.
21. M. Andres-Vergés and S. J. Serna, *J. Mater. Sci. Lett.* **7** (1988) 970–972.
22. M. Andres-Vergés, A. Mifsud, and C. J. Serna, *J. Chem. Soc., Faraday Trans.* **86** (1990) 959–963.
23. T. Pandiyarajan, R. Udayabhaskar, and B. Karthikeyan, *Appl. Phys. A* **107** (2012) 411–419.
24. F. Ahmed, S. Kumar, N. Arshi, M. S. Anwar, B. H. Koo, and C. G. Lee, *Microelectron. Eng.* **89** (2012) 129–132.
25. S. K. Kansal, A. H. Ali, S. Kapoor, and D. W. Bahnemann, *Sep. Purif. Technol.* **80** (2011) 125–130.
26. X. Sui, Y. Liu, C. Shao, Y. Liu, and C. Xu, *Chem. Phys. Lett.* **424** (2006) 340–344.
27. T. C. Damen, S. P. S. Porto, and B. Tell, *Phys. Rev.* **142** (1966) 570–573.
28. M. Ristić, M. Ivanda, S. Popović, and S. Musić, *J. Non-Cryst. Solids* **303** (2012) 270–280.
29. J. Zhao, X. Yan, Y. Yang, Y. Huang, and Y. Zhang, *Mater. Lett.* **64** (2010) 569–572.
30. A. Stanković, Z. Stojanović, Lj. Veselinović, S. D. Škapin, I. Bračko, S. Marković, and D. Uskoković, *Mater. Sci. Eng. B* **177** (2012) 1038–1045.